Deformable Image Registration with Implicit Neural Representations

Seminar: Deep Learning for Medical Applications

Tutor: Magdalena Wysocki

Student: Xingyu Zhang

Date: 4 Jul. 2024

Technische Universität München + Johns Hopkins Whiting School of Engineering

Introduction

Technische Universität München + Johns Hopkins Whiting School of Engineering

Problem of Interest

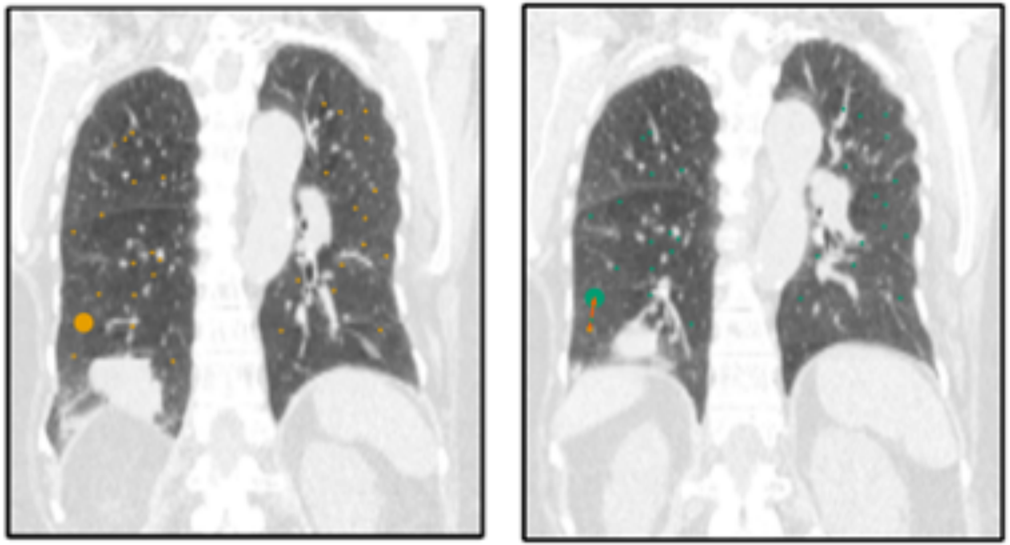

Images adapted from [1]

Can we find the matching point between images?

[1] J. M. Wolterink, J. C. Zwienenberg, and C. Brune. “Implicit neural representations for deformable image registration”. In: International Conference on Medical Imaging with Deep Learning . PMLR. 2022, pp. 1349– 1359.

Deformable Image Registration

- Aligning corresponding semantic regions across images
- Non-rigid deformations

- **Applications**
  - Motion analysis
  - Multi-modal image analysis
  - Disease tracking

Deformable Image Registration

- **Conventional Iterative Methods**: mathematical modals
    - Effective
    - High computational resources
    - Sensitive to noise

- **Data-driven Methods**: deep learning architectures
    - Fast inference
    - Reduced accuracy
    - Large training data
    - Resolution dependency
    - Generalization failure

Implicit Neural Representations (INRs)

- Implicitly represent continuous signals as a function stored in the weights of a multi-layer perceptron [2]

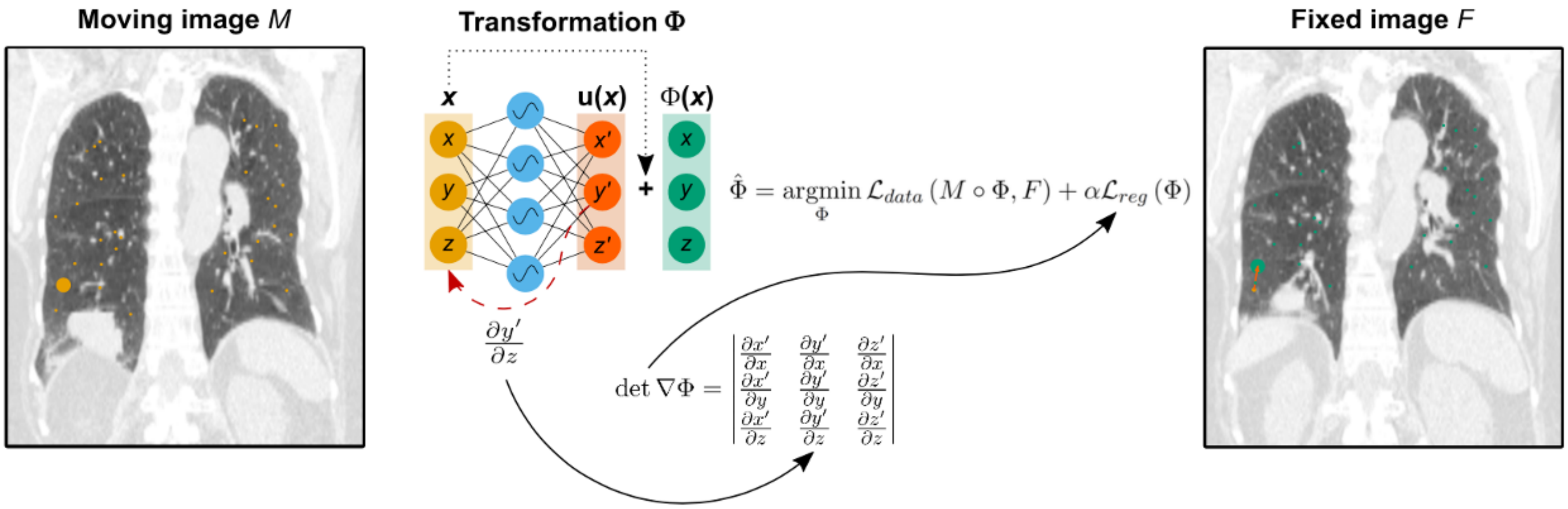

Schematic Overview of INRs for Image Registration [1]

[1] J. M. Wolterink, J. C. Zwienenberg, and C. Brune. "Implicit neural representations for deformable image registration". In: International Conference on Medical Imaging with Deep Learning . PMLR. 2022, pp. 1349– 1359.
[2] V. Sitzmann, J. Martel, A. Bergman, D. Lindell, and G. Wetzstein. "Implicit neural representations with periodic activation functions". In: Advances in neural information processing systems 33 (2020), pp. 7462–7473.

Implicit Neural Representations (INRs)

- **Advantages**
  - Continuous representation
  - Memory efficiency
  - Accurate gradients
  - Pair-wise optimization

- **Challenges**
  - Complex deformations
  - Spatial folding
  - Failure due to non-convex optimization

➡ **Motivation**

CAMP

Paper Summaries

Technische Universität München

Johns Hopkins
Whiting School
of Engineering

Geometry-Informed INRs [3]

Research Problem

Complex deformations ➡ Simplify deformation function via geometric alignment

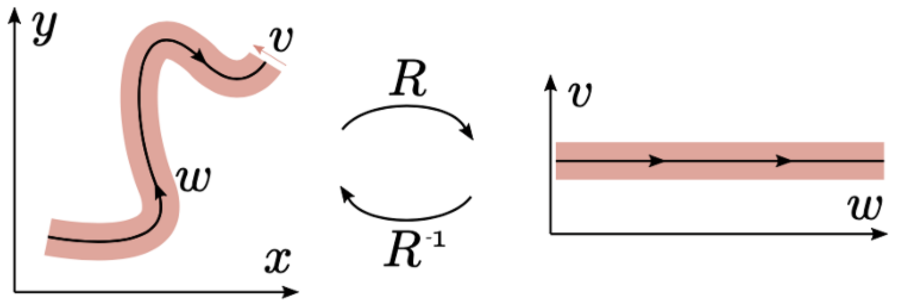

Source [3]

Geometry-Informed INRs

Method

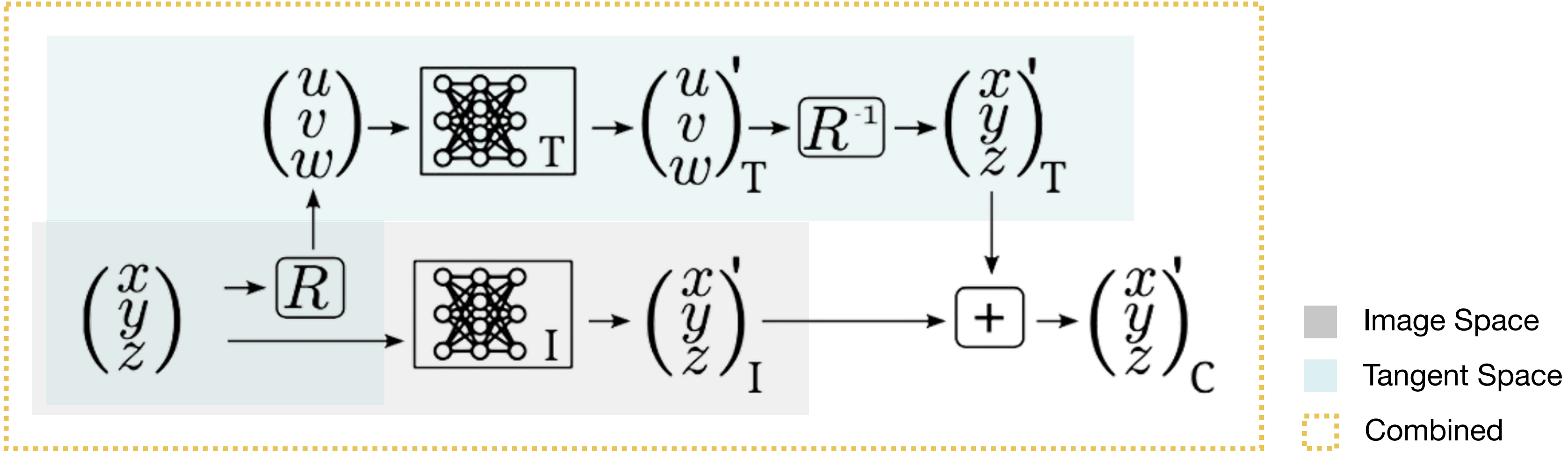

Image adapted from [3]

Geometry-Informed INRs

Experiments & Results: Quantitative

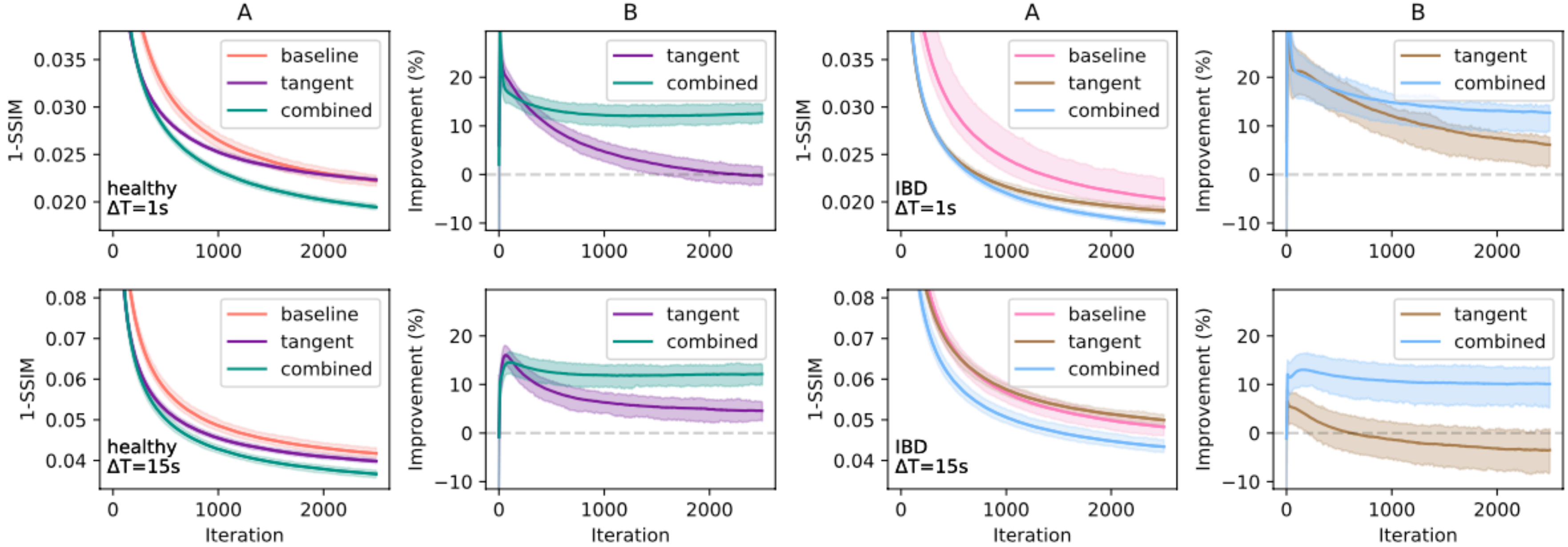

Source [3]

[3] L. van Harten, R. L. M. Van Herten, J. Stoker, and I. Isgum. “Deformable Image Registration with Geometry-informed Implicit Neural Representations”. In: Medical Imaging with Deep Learning . PMLR. 2024, pp. 730– 742.

Geometry-Informed INRs

Experiments & Results: Qualitative

Bowel motility as dominant motion ➡ beneficial

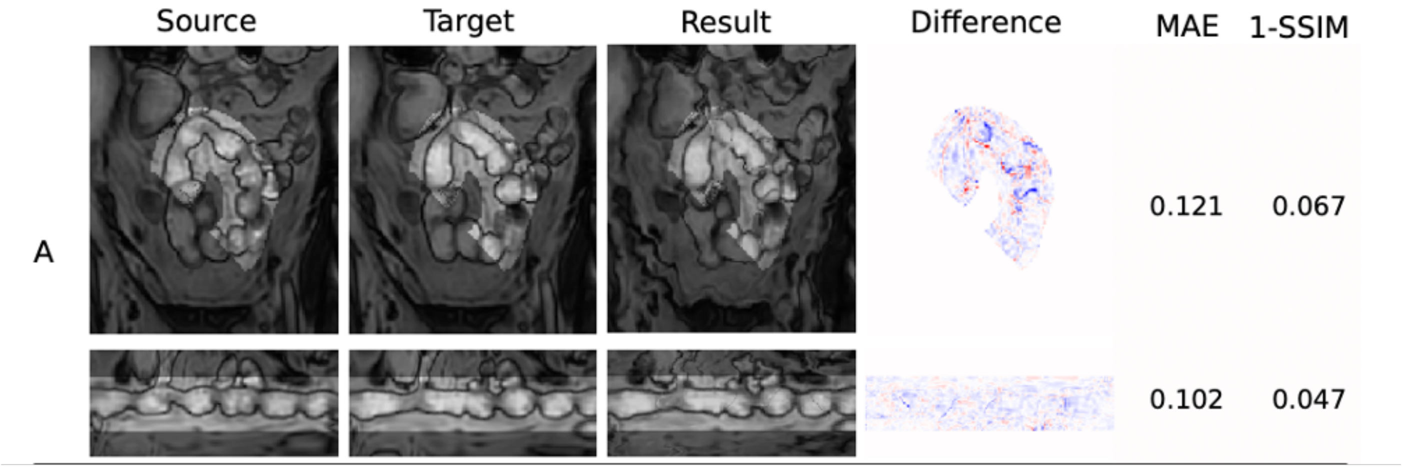

Image adapted from [3]

[3] L. van Harten, R. L. M. Van Herten, J. Stoker, and I. Isgum. “Deformable Image Registration with Geometry-informed Implicit Neural Representations”. In: Medical Imaging with Deep Learning . PMLR. 2024, pp. 730– 742.

Geometry-Informed INRs

Experiments & Results: Qualitative

- Centerline inaccurately extracted
- Motility absent

➡ not beneficial

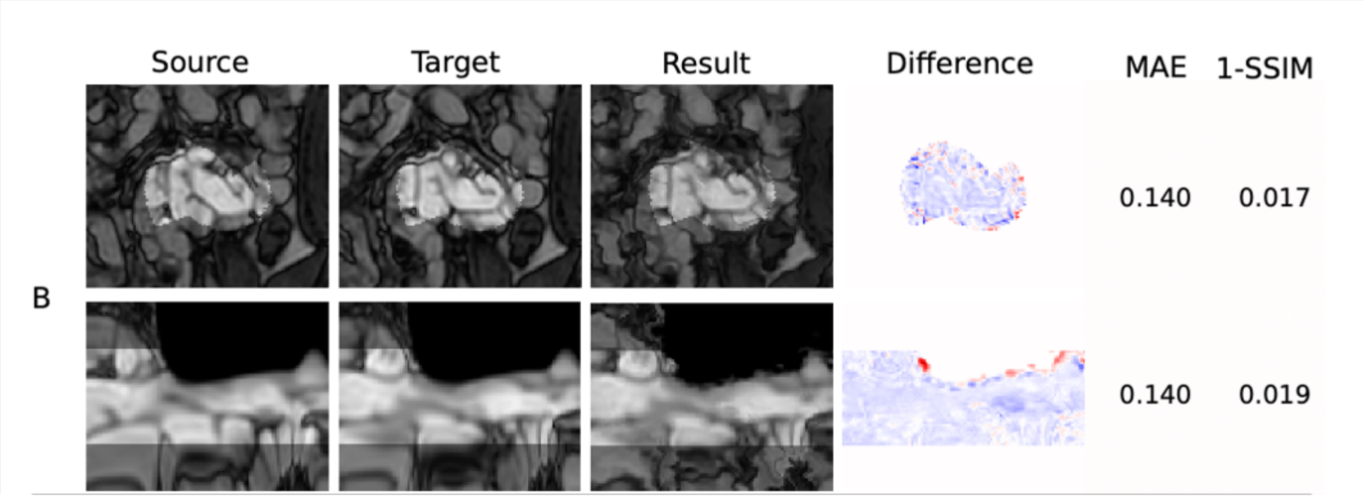

Image adapted from [3]

[3] L. van Harten, R. L. M. Van Herten, J. Stoker, and I. Isgum. “Deformable Image Registration with Geometry-informed Implicit Neural Representations”. In: Medical Imaging with Deep Learning . PMLR. 2024, pp. 730– 742.

Geometry-Informed INRs

Experiments & Results: Qualitative

Breathing becomes the dominant motion ➡ harmful

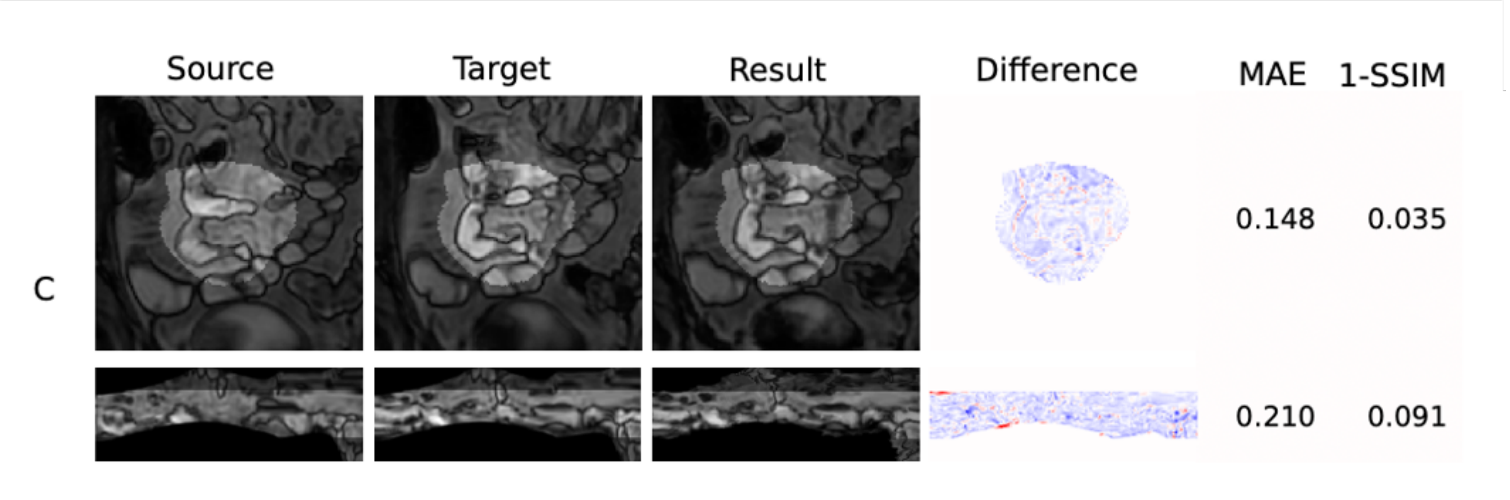

Image adapted from [3]

[3] L. van Harten, R. L. M. Van Herten, J. Stoker, and I. Isgum. "Deformable Image Registration with Geometry-informed Implicit Neural Representations". In: Medical Imaging with Deep Learning . PMLR. 2024, pp. 730– 742.

Geometry-Informed INRs [3]

Discussion

- **Advantages**
  - improved registration accuracy for bowel loops with active motility;
  - accuracy further improved with the combined model;
  - improved efficiency;
  - potential application in other areas, e.g. cardiac motion, ischemic stroke follow-up
- **Limitations**
  - additional resources for centerline extraction;
  - limited / negative impact due to bad centerline extraction or dominant breathing motion;
  - generalisability questionable without further test;

SINR: Spline-enhanced INR [4]

Research Problem

- Spatial folding
- Sampling method not optimal for multi-modal registration

➔ Combining B-spline Free Form Deformation (FFD) [5] with INRs for smooth transformations

[4] V. Sideri-Lampretsa, J. McGinnis, H. Qiu, M. Paschali, W. Simson, and D. Rueckert. “SINR: Spline-enhanced implicit neural representation for multi-modal registration”. In: Medical Imaging with Deep Learning . 2024.
[5] D. Rueckert, L. I. Sonoda, C. Hayes, D. L. Hill, M. O. Leach, and D. J. Hawkes. “Nonrigid registration using free-form deformations: application to breast MR images”. In: IEEE transactions on medical imaging 18.8 (1999), pp. 712–721.

SINR: Spline-enhanced INR

Method: FFD

- Control points
- B-spline basis functions
- Smooth deformations

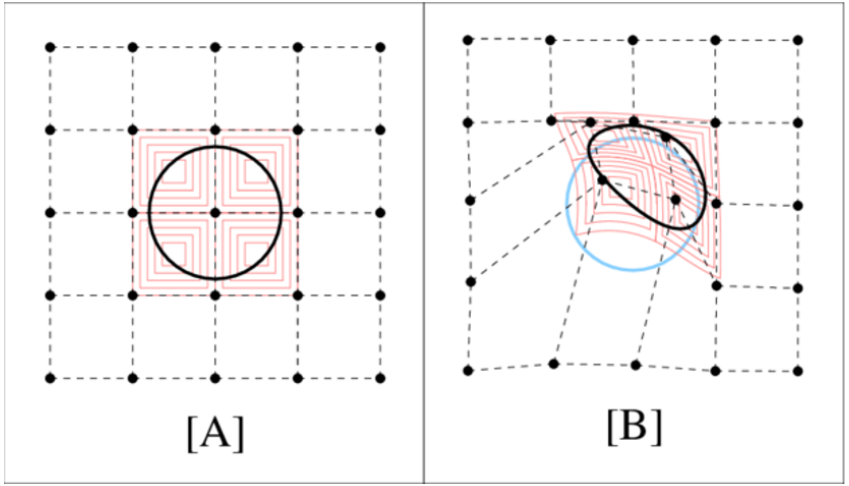

Image adapted from [6]

[6] J. E. Gain. Enhancing spatial deformation for virtual sculpting. Tech. rep. University of Cambridge, Computer Laboratory, 2000.

SINR: Spline-enhanced INR

Method: Schematic Overview

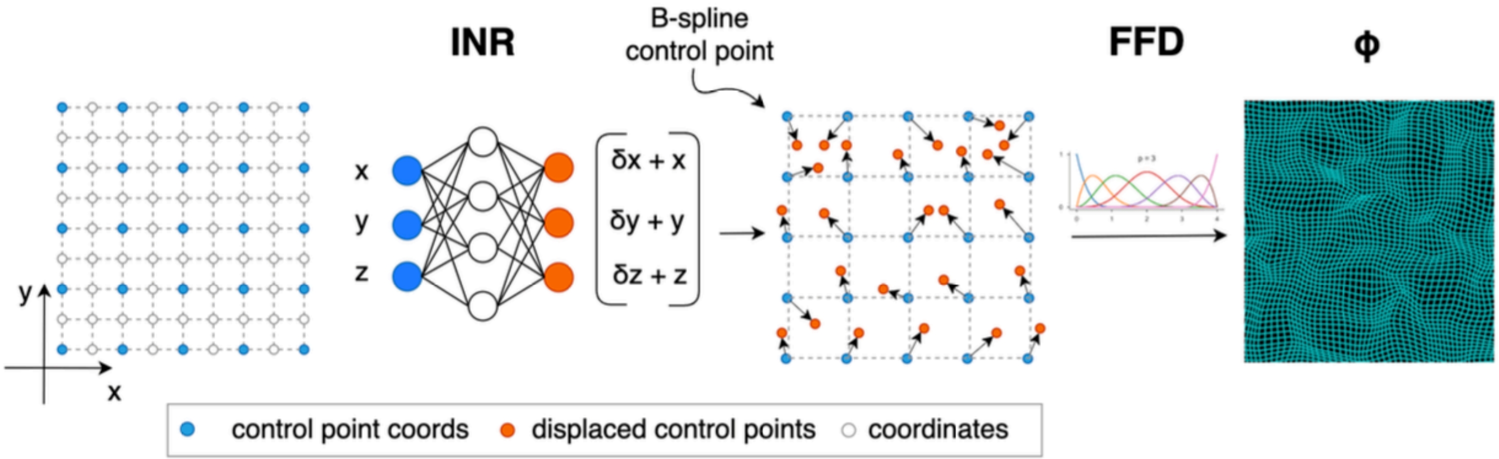

Source [4]

SINR: Spline-enhanced INR

Experiments & Results: Quantitative Overview

		T1w-T1w CamCAN		T1w-T2w CamCAN	
Method	FFD	Dice $\pm$ std $\uparrow$	Folding % $\downarrow$	Dice $\pm$ std $\uparrow$	Folding % $\downarrow$
Affine	n/a	0.619 ± 0.01	-	0.619 ± 0.01	-
MIRTK	✓	0.833 ± 0.02	0.11	0.755 ± 0.01	0.14
VMorph [CNN]	✗	0.812 ± 0.06	0.31	0.733 ± 0.04	0.19
MIDIR [CNN]	✓	0.817 ± 0.06	0.23	0.735 ± 0.04	0.12
IDIR [ReLU-MLP]	✗	0.806 ± 0.02	0.44	0.683 ± 0.03	0.15
SINR [ReLU-MLP]	✓	0.789 ± 0.03	0.38	0.721 ± 0.06	0.05
IDIR [SIREN]	✗	0.837 ± 0.05	0.84	0.736 ± 0.02	0.81
SINR [SIREN]	✓	$\mathbf{0.855 \pm 0.06}$	0.59	$\mathbf{0.784 \pm 0.04}$	0.27

Source [4]

[4] V. Sideri-Lampretsa, J. McGinnis, H. Qiu, M. Paschali, W. Simson, and D. Rueckert. “SINR: Spline-enhanced implicit neural representation for multi-modal registration”. In: Medical Imaging with Deep Learning . 2024.

SINR: Spline-enhanced INR

Experiments & Results: Quantitative by Structure

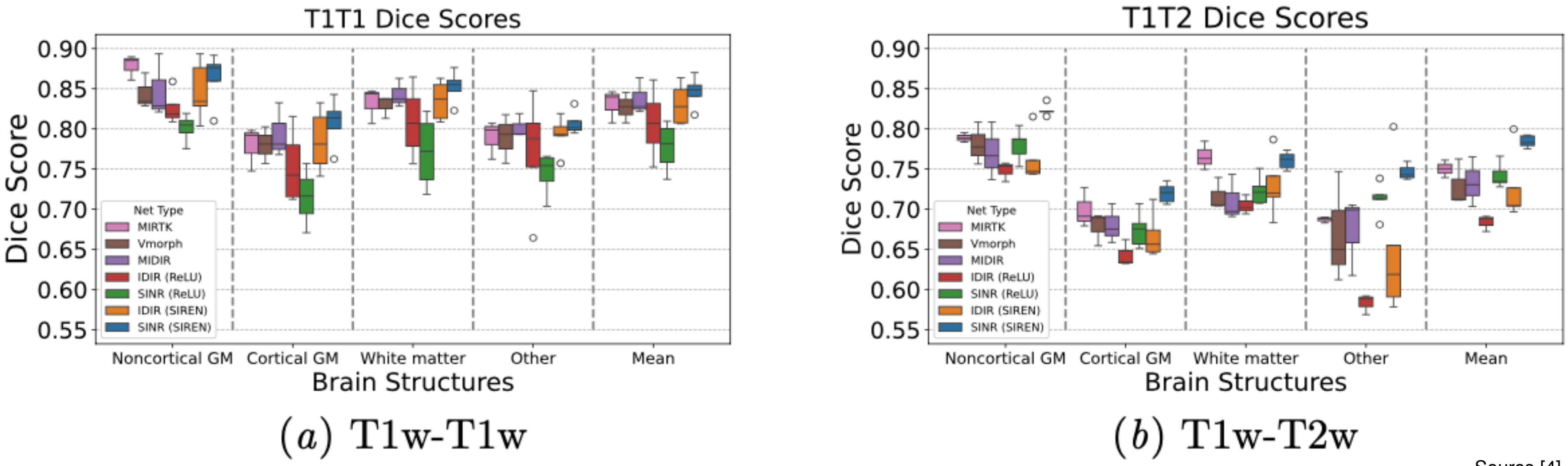

Source [4]

[4] V. Sideri-Lampretsa, J. McGinnis, H. Qiu, M. Paschali, W. Simson, and D. Rueckert. “SINR: Spline-enhanced implicit neural representation for multi-modal registration”. In: Medical Imaging with Deep Learning . 2024.

SINR: Spline-enhanced INR

Experiments & Results: Qualitative

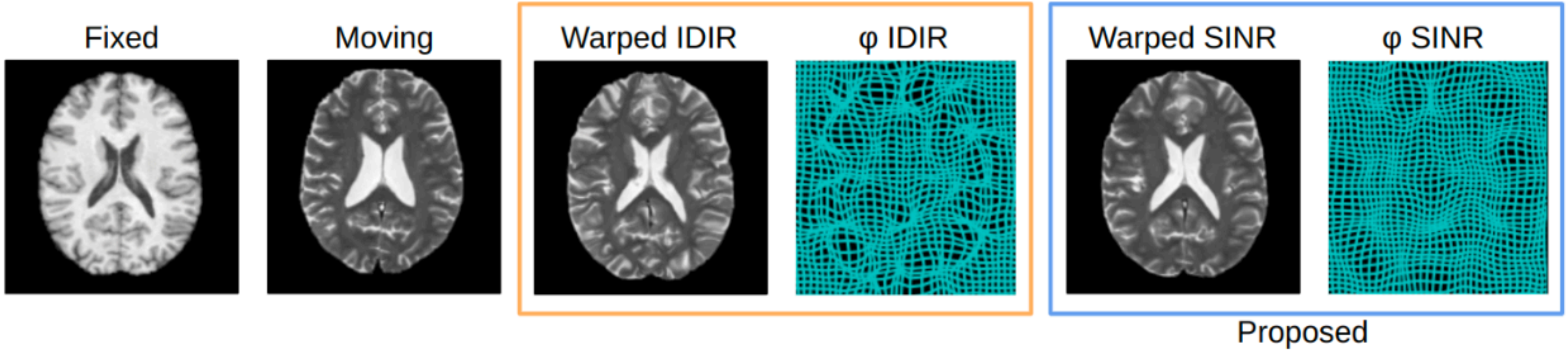

Source [4]

[4] V. Sideri-Lampretsa, J. McGinnis, H. Qiu, M. Paschali, W. Simson, and D. Rueckert. “SINR: Spline-enhanced implicit neural representation for multi-modal registration”. In: Medical Imaging with Deep Learning . 2024.

SINR: Spline-enhanced INR

Discussion

- **Advantages**
  - higher Dice score than existing methods;
  - reduced folding ratio for INR-based method;
  - efficient spatial sampling and calculation of metrics for multi-modal registration.

- **Limitations**
  - higher folding ratio compared to conventional and CNN-based methods;
  - balance between the accuracy and folding ratio yet to be explored;
  - generalisability questionable without further test.

Cycle-Consistent INRs [7]

Research Problem

- Failure due to non-convex optimization
- Sensitive to initialization settings

➡ Using forward-backward cycle-consistency to improve robustness

Cycle-Consistent INRs

Method: Optimization

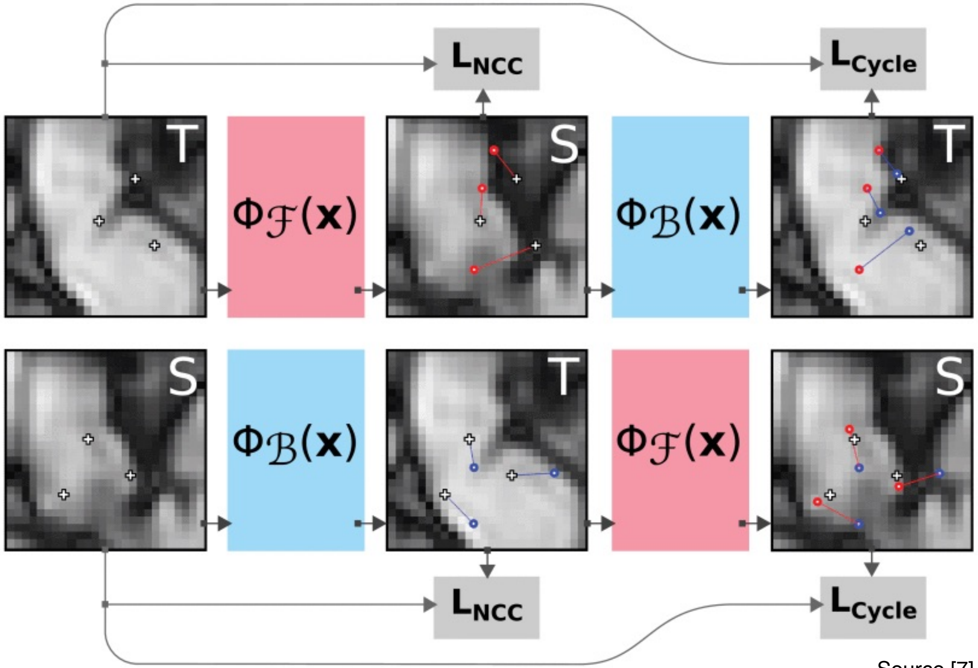

Source [7]

[7] L. D. Van Harten, J. Stoker, and I. I˘sgum. "Robust deformable image registration using cycle-consistent implicit representations". In: IEEE Transactions on Medical Imaging (2023).

Cycle-Consistent INRs

Method: Inference

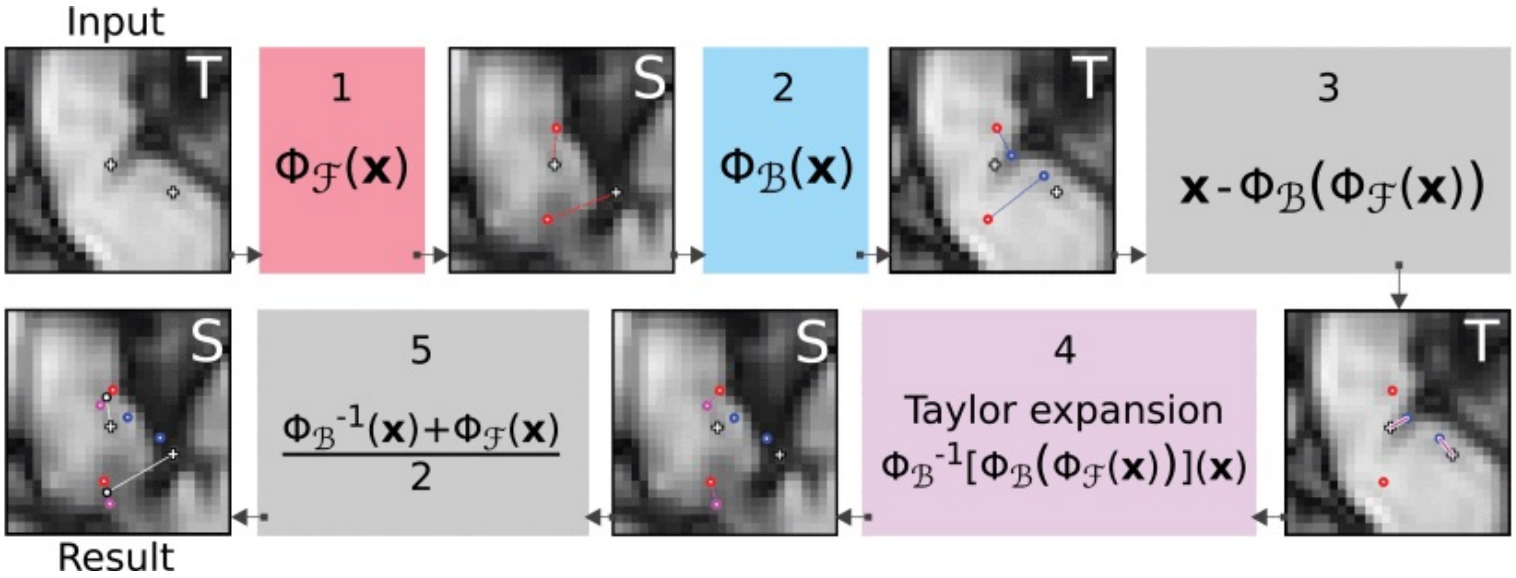

Source [7]

[7] L. D. Van Harten, J. Stoker, and I. I˘sgum. “Robust deformable image registration using cycle-consistent implicit representations”. In: IEEE Transactions on Medical Imaging (2023).

Cycle-Consistent INRs

Experiments & Results: Lung CT Data

Method	mean ± std (mm)
DLIR [7]	2.64 ± 4.32
VoxelMorph [8]	2.26 ± 2.30
CycleMorph [21]	2.19 ± 2.26
CNN with anatomical constraints [29]	1.14 ± 0.76
Uniform B-Splines [30]	1.36 ± 1.01
CorrField [31]	1.12 ± 1.08
Keypoint correspondence optimization [32]	0.94 ± 1.06
● INR + Symmetric Jacobian det.	1.27 ± 2.27
● INR + Bending penalty	1.10 ± 1.42
● INR + Symmetric Jacobian det. + cycle	1.04 ± 1.11
● INR + Bending penalty + cycle	1.06 ± 1.34

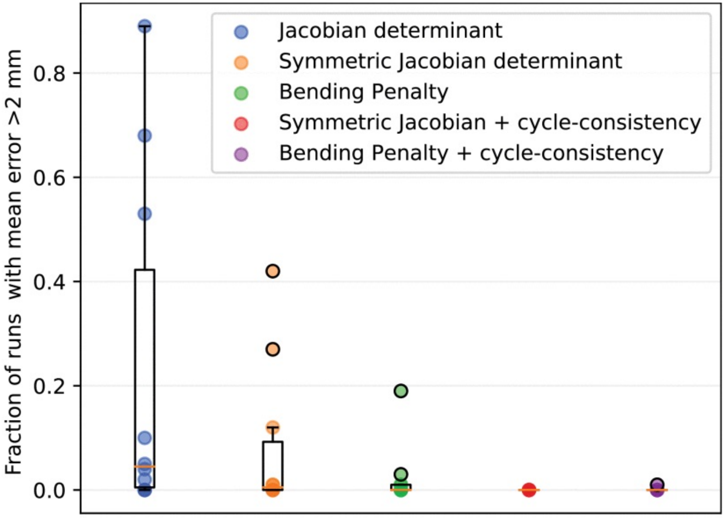

Source [7]

Cycle-Consistent INRs

Experiments & Results: Sensitivity to Hyperparameters

Setting	TRE (mm)	Failure rate (%)
Single INR ($\alpha = 0.05$, $\beta = 0$)	1.14	8.3
Proposed ($\alpha = 0.05$, $\beta = 1e{-}3$)	1.07	0
Jacobian det. $\alpha = 0.50$	1.11	0
Jacobian det. $\alpha = 0.10$	1.08	0
Jacobian det. $\alpha = 0.025$	1.07	0.3
Jacobian det. $\alpha = 0.005$	1.07	1.8
cycle $\beta = 1e{-}2$	1.08	0.4
cycle $\beta = 2e{-}3$	1.07	0
cycle $\beta = 5e{-}4$	1.07	0
cycle $\beta = 1e{-}4$	1.06	0.4
ReLU network	1.22	0
No masks	1.11	0

Source [7]

[7] L. D. Van Harten, J. Stoker, and I. I˘sgum. “Robust deformable image registration using cycle-consistent implicit representations”. In: IEEE Transactions on Medical Imaging (2023).

Cycle-Consistent INRs

Experiments & Results: Abdominal MRI Data

T_0

T_{15} Single INR

T_{15} Proposed

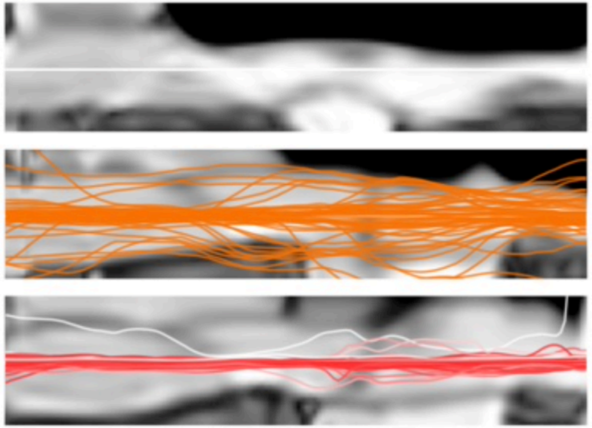

Strategy	Discrepancy (mm) ± stdev 1s	5s	10s	15s
Single INR	0.68 ± 0.68	2.26 ± 2.05	2.47 ± 2.05	2.99 ± 2.31
Proposed	0.45 ± 0.54	1.21 ± 1.06	1.48 ± 1.54	1.62 ± 1.57

Source [7]

[7] L. D. Van Harten, J. Stoker, and I. Iˇsgum. “Robust deformable image registration using cycle-consistent implicit representations”. In: IEEE Transactions on Medical Imaging (2023).

Cycle-Consistent INRs

Discussion

- **Advantages**
  - significantly improved registration accuracy and robustness;
  - insensitive to hyperparameter settings;
  - introduces an uncertainty metric useful for automatic quality control;
  - generalisability tested on two different datasets;
  - discussed possible changes for multi-modal registration.

- **Limitations**
  - higher computational complexity and runtime;
  - limited application with high dimensional data and in real-time applications.

Conclusion

Conclusion

Summary

Challenge	Approach	Accuracy	Efficiency	Generalisibility
Complex deformations	Geometric prior	+	+	Untested
Spatial folding	Spline-based FFD	+	-	Untested
Optimization failure	Cycle-consistency	+	-	Tested

Conclusion

Future Works

If generalization of INRs can further improve the registration performance?

- General or statistical representation of a structure
- Statistical atlas as regularizer
- Complementary data sources

Thank You for Your Attention

Q & A

Technische Universität München

JOHNS HOPKINS
WHITING SCHOOL
of ENGINEERING

Bibliography

[1] J. M. Wolterink, J. C. Zwienenberg, and C. Brune. “Implicit neural representations for deformable image registration”. In: International Conference on Medical Imaging with Deep Learning . PMLR. 2022, pp. 1349– 1359.

[2] V. Sitzmann, J. Martel, A. Bergman, D. Lindell, and G. Wetzstein. “Implicit neural representations with periodic activation functions”. In: Advances in neural information processing systems 33 (2020), pp. 7462–7473.

[3] L. van Harten, R. L. M. Van Herten, J. Stoker, and I. Isgum. “Deformable Image Registration with Geometry-informed Implicit Neural Representations”. In: Medical Imaging with Deep Learning . PMLR. 2024, pp. 730– 742.

[4] V. Sideri-Lampretsa, J. McGinnis, H. Qiu, M. Paschali, W. Simson, and D. Rueckert. “SINR: Spline-enhanced implicit neural representation for multi-modal registration”. In: Medical Imaging with Deep Learning . 2024.

[5] D. Rueckert, L. I. Sonoda, C. Hayes, D. L. Hill, M. O. Leach, and D. J. Hawkes. “Nonrigid registration using free-form deformations: application to breast MR images”. In: IEEE transactions on medical imaging 18.8 (1999), pp. 712–721.

[6] J. E. Gain. Enhancing spatial deformation for virtual sculpting. Tech. rep. University of Cambridge, Computer Laboratory, 2000.

[7] L. D. Van Harten, J. Stoker, and I. Iˇsgum. “Robust deformable image registration using cycle-consistent implicit representations”. In: IEEE Transactions on Medical Imaging (2023).

[8] M. Dannecker, V. Kyriakopoulou, L. Cordero-Grande, A. N. Price, J. V. Hajnal, and D. Rueckert. “CINA: Conditional Implicit Neural Atlas for Spatio-Temporal Representation of Fetal Brains”. In: arXiv preprint arXiv:2403.08550 (2024).

[9] G. Balakrishnan, A. Zhao, M. R. Sabuncu, J. Guttag, and A. V. Dalca. “Voxelmorph: a learning framework for deformable medical image registration”. In: IEEE transactions on medical imaging 38.8 (2019), pp. 1788– 1800.

Supplemental Slides

Technische Universität München

Johns Hopkins
Whiting School of Engineering

Geometry-Informed INRs

Method: Loss Function

$$
\begin{aligned}
L &= L^{data} + \alpha L^{jac} \\
&= \frac{1}{bs} \sum_{i=1}^{bs} \left(-NCC \left(T[R^{-1}(\bar{x}_i)], S[R^{-1}(\Phi(\bar{x}_i))] \right) + \alpha \left| 1 - \det \nabla \Phi[\bar{x}_i] \right| \right),
\end{aligned}
$$

[3] L. van Harten, R. L. M. Van Herten, J. Stoker, and I. Isgum. "Deformable Image Registration with Geometry-informed Implicit Neural Representations". In: Medical Imaging with Deep Learning . PMLR. 2024, pp. 730– 742.

SINR: Spline-enhanced INR

Method: FFD

$$\mathbf{u}(x,y,z) = \sum_{l=0}^{3}\sum_{m=0}^{3}\sum_{n=0}^{3} B_l(u)B_m(v)B_n(w)c_{i+l}c_{j+m}c_{k+n},$$

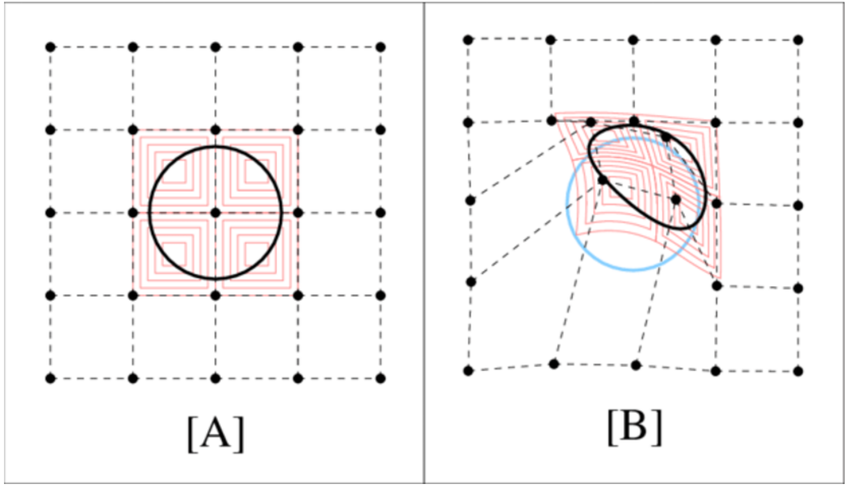

Image adapted from [6]

B-spline Basis Functions [5]:

$$B_0(u) = \frac{(1-u)^3}{6}, \quad B_1(u) = \frac{3u^3 - 6u^2 + 4}{6},$$
$$B_2(u) = \frac{-3u^3 + 3u^2 + 3u + 1}{6}, \quad B_3(u) = \frac{u^3}{6}$$

[5] D. Rueckert, L. I. Sonoda, C. Hayes, D. L. Hill, M. O. Leach, and D. J. Hawkes. “Nonrigid registration using free-form deformations: application to breast MR images”. In: IEEE transactions on medical imaging 18.8 (1999), pp. 712–721.
[6] J. E. Gain. Enhancing spatial deformation for virtual sculpting. Tech. rep. University of Cambridge, Computer Laboratory, 2000.

SINR: Spline-enhanced INR

Experiments & Results: Sensitivity to Hyperparameter

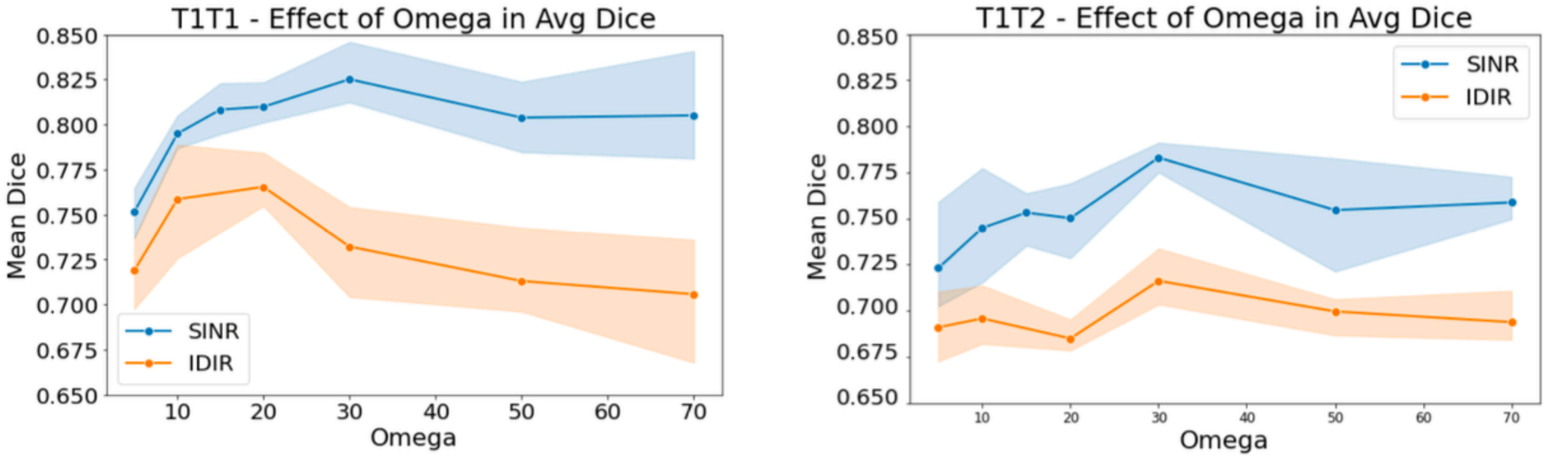

(a) T1w-T1w

(b) T1w-T2w

Source [4]

[4] V. Sideri-Lampretsa, J. McGinnis, H. Qiu, M. Paschali, W. Simson, and D. Rueckert. “SINR: Spline-enhanced implicit neural representation for multi-modal registration”. In: Medical Imaging with Deep Learning . 2024.

SINR: Spline-enhanced INR

Experiments & Results: Run Time

Table 2: Runtime for mono- and multi-modal registration for all methods.

	Runtime↓	
Method	T1w-T1w CamCAN	T1w-T2w CamCAN
MIRTK	3min 28s	3min 41s
VMorph [CNN]	**Train:** 15h 23min **Test:** 219ms	**Train:** 15h 34min **Test:** 219ms
MIDIR [CNN]	**Train:** 12h 55min **Test:** 113ms	**Train:** 12h 49min **Test:** 113ms
IDIR [ReLU-MLP]	**Fit:** 1min 43s **Test:** 2.9s	**Fit:**2min 01s **Test:** 2.9s
SINR [ReLU-MLP]	**Fit:** 1min 54s **Test:** 2.9s	**Fit:** 2min 17s **Test:** 2.9s
IDIR [SIREN]	**Fit:** 45s **Test:** 2.9s	**Fit:** 1min 39s **Test:** 2.9s
SINR [SIREN]	**Fit:** 1min 32s **Test:** 2.9s	**Fit:** 2min 12s **Test:** 2.9s

Source [4]

[4] V. Sideri-Lampretsa, J. McGinnis, H. Qiu, M. Paschali, W. Simson, and D. Rueckert. “SINR: Spline-enhanced implicit neural representation for multi-modal registration”. In: Medical Imaging with Deep Learning . 2024.

Cycle-Consistent INRs

Method: Optimization

$$L_{\text{total}} = L_{\mathcal{F}}^{data} + \alpha L_{\phi_{\mathcal{F}}}^{reg} + \beta L_{\mathcal{F}\to\mathcal{B}}^{cycle} + L_{\mathcal{B}}^{data} + \alpha L_{\phi_{\mathcal{B}}}^{reg} + \beta L_{\mathcal{B}\to\mathcal{F}}^{cycle},$$

$$L_{\mathcal{F}}^{\text{data}} = \frac{2}{bs} \sum_{i=1}^{bs/2} -\text{NCC}(S[\vec{x}_i], T[\Phi_{\mathcal{F}}(\vec{x}_i)]),$$

$$L^{sjac}[\Phi] = \frac{1}{bs} \sum_{i=1}^{bs} \min\left(\frac{(\det \nabla\Phi[\vec{x}_i] - 1)^2}{\det \nabla\Phi[\vec{x}_i]}, \tau \right),$$

$$L_{\mathcal{F}\to\mathcal{B}}^{cycle} = \frac{2}{bs} \sum_{i=1}^{bs/2} [\Phi_{\mathcal{B}}(\Phi_{\mathcal{F}}(\vec{x}_i)) - \vec{x}_i]^2$$

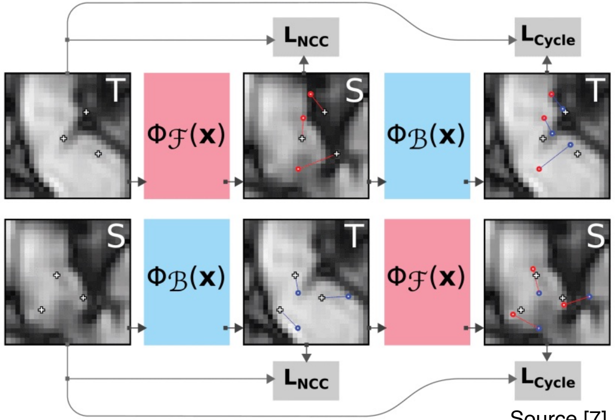

Source [7]

[7] L. D. Van Harten, J. Stoker, and I. I˘sgum. “Robust deformable image registration using cycle-consistent implicit representations”. In: IEEE Transactions on Medical Imaging (2023).

Cycle-Consistent INRs

Method: Complete Backward and Forward Terms

Data Loss:

$$L_{\mathcal{F}}^{\text{data}} = \frac{2}{bs} \sum_{i=1}^{bs/2} -\text{NCC}(S[\vec{x}_i], T[\Phi_{\mathcal{F}}(\vec{x}_i)]),$$

$$L_{\mathcal{B}}^{\text{data}} = \frac{2}{bs} \sum_{i=bs/2}^{bs} -\text{NCC}(T[\vec{x}_i], S[\Phi_{\mathcal{B}}(\vec{x}_i)]),$$

Cycle-consistent Terms:

$$L_{\mathcal{F}\to\mathcal{B}}^{cycle} = \frac{2}{bs} \sum_{i=1}^{bs/2} [\Phi_{\mathcal{B}}(\Phi_{\mathcal{F}}(\vec{x}_i)) - \vec{x}_i]^2$$

$$L_{\mathcal{B}\to\mathcal{F}}^{cycle} = \frac{2}{bs} \sum_{i=bs/2}^{bs} [\Phi_{\mathcal{F}}(\Phi_{\mathcal{B}}(\vec{x}_i)) - \vec{x}_i]^2,$$

[7] L. D. Van Harten, J. Stoker, and I. I˘sgum. “Robust deformable image registration using cycle-consistent implicit representations”. In: IEEE Transactions on Medical Imaging (2023).

Cycle-Consistent INRs

Method: Complete Regularization Tested

Jacobian determinant regularization:

$$L^{jac}[\Phi] = \frac{1}{bs}\sum_{i=1}^{bs} |1 - \det \nabla\Phi[\bar{x}_i]|.$$

Symmetric Jacobian determinant regularization:

$$L^{sjac}[\Phi] = \frac{1}{bs}\sum_{i=1}^{bs} \min\left(\frac{(\det \nabla\Phi[\vec{x}_i] - 1)^2}{\det \nabla\Phi[\vec{x}_i]}, \tau\right),$$

Bending Energy Penalty [5]:

$$\begin{aligned} L^{bend}[\Phi] \\ = \frac{1}{bs}\sum_{i=1}^{bs} \Bigg(&\left(\frac{\partial^2\Phi[\bar{x}_i]}{\partial x^2}\right)^2 + \left(\frac{\partial^2\Phi[\bar{x}_i]}{\partial y^2}\right)^2 + \left(\frac{\partial^2\Phi[\bar{x}_i]}{\partial z^2}\right)^2 \\ &+ 2\left[\left(\frac{\partial^2\Phi[\bar{x}_i]}{\partial x \partial y}\right)^2 + \left(\frac{\partial^2\Phi[\bar{x}_i]}{\partial x \partial z}\right)^2 + \left(\frac{\partial^2\Phi[\bar{x}_i]}{\partial y \partial z}\right)^2\right]\Bigg), \end{aligned}$$

[5] D. Rueckert, L. I. Sonoda, C. Hayes, D. L. Hill, M. O. Leach, and D. J. Hawkes. “Nonrigid registration using free-form deformations: application to breast MR images”. In: IEEE transactions on medical imaging 18.8 (1999), pp. 712–721.
[7] L. D. Van Harten, J. Stoker, and I. I˘sgum. “Robust deformable image registration using cycle-consistent implicit representations”. In: IEEE Transactions on Medical Imaging (2023).

Cycle-Consistent INRs

Method: Inference – Tayler Expansion

$$
\begin{aligned}
\Phi_{\mathcal{B}}^{-1}(\vec{x}) =& \Phi_{\mathcal{B}}^{-1}[\Phi_{\mathcal{B}}(\Phi_{\mathcal{F}}(\vec{x}))]+ \\
& \nabla\Phi_{\mathcal{B}}^{-1}[\Phi_{\mathcal{B}}(\Phi_{\mathcal{F}}(\vec{x}))] \cdot (\vec{x} - \Phi_{\mathcal{B}}(\Phi_{\mathcal{F}}(\vec{x}))+ \\
& \frac{1}{2}\nabla^2\Phi_{\mathcal{B}}^{-1}[\Phi_{\mathcal{B}}(\Phi_{\mathcal{F}}(\vec{x}))] \cdot (\vec{x} - \Phi_{\mathcal{B}}(\Phi_{\mathcal{F}}(\vec{x})))^2.
\end{aligned}
$$

Can be simplied to:

$$
\begin{aligned}
\Phi_{\mathcal{B}}^{-1}(\vec{x}) =& \Phi_{\mathcal{F}}(\vec{x})+ \\
& \nabla^{-1}\Phi_{\mathcal{B}}(\Phi_{\mathcal{F}}(\vec{x})) \cdot (\vec{x} - \Phi_{\mathcal{B}}(\Phi_{\mathcal{F}}(\vec{x})))+ \\
& \frac{1}{2}\nabla^{-2}\Phi_{\mathcal{B}}(\Phi_{\mathcal{F}}(\vec{x})) \cdot (\vec{x} - \Phi_{\mathcal{B}}(\Phi_{\mathcal{F}}(\vec{x})))^2,
\end{aligned}
$$

[7] L. D. Van Harten, J. Stoker, and I. I˘sgum. “Robust deformable image registration using cycle-consistent implicit representations”. In: IEEE Transactions on Medical Imaging (2023).

CINA: Conditional Implicit Neural Atlas

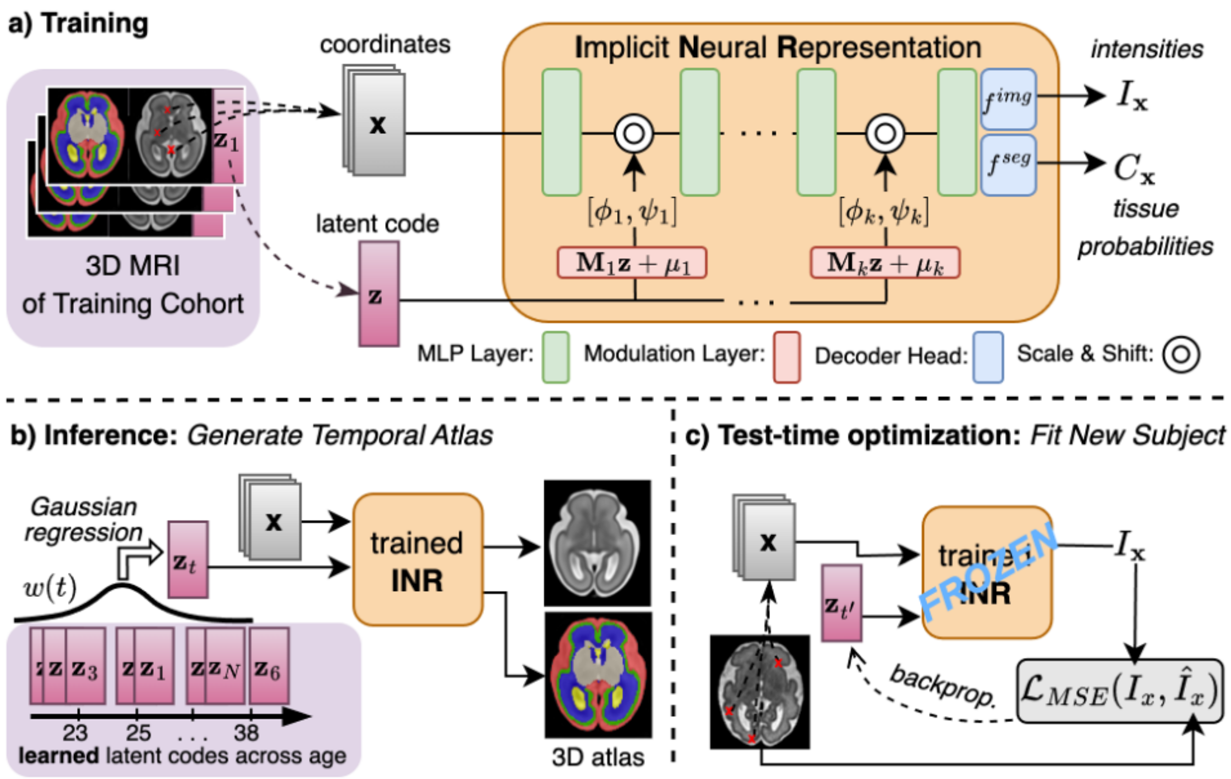

Source [8]